Open Access

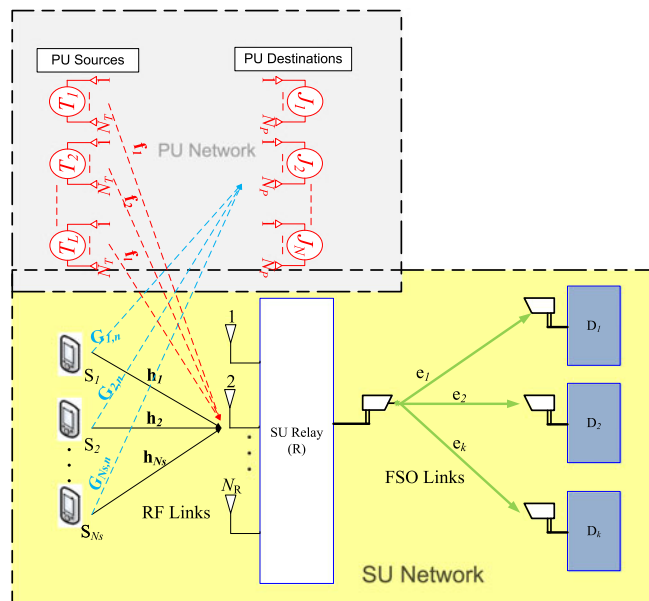# Outage Analysis of Mixed Underlay Cognitive RF MIMO and FSO Relaying With Interference Reduction

**Fawaz S. Al-Qahtani,** *Member, IEEE*
**Ahmed H. Abd El-Malek,** *Member, IEEE*
**Imran S. Ansari,** *Member, IEEE*
**Redha M. Radaydeh,** *Senior Member, IEEE*
**Salam A. Zummo,** *Senior Member, IEEE*

# Outage Analysis of Mixed Underlay Cognitive RF MIMO and FSO Relaying With Interference Reduction

**Fawaz S. Al-Qahtani,**[1] *Member, IEEE,*
**Ahmed H. Abd El-Malek,**[2] *Member, IEEE,*
**Imran S. Ansari,**[1] *Member, IEEE,*
**Redha M. Radaydeh,**[3] *Senior Member, IEEE,*
**and Salam A. Zummo,**[4] *Senior Member, IEEE*

[1]Electrical and Computer Engineering Program, Texas A&M University at Qatar, Doha 23874, Qatar
[2]Department of Electrical Engineering, Pharos University in Alexandria, Alexandria, Egypt
[3]Computer, Electrical, and Mathematical Sciences and Engineering Division, King Abdullah University of Science and Technology, Thuwal 23955-6900, Saudi Arabia
[4]Department of Electrical Engineering, King Fahd University of Petroleum and Minerals, Dharan 34463 31261, Saudi Arabia

**Abstract:** In this paper, we study the outage performance of multiuser mixed underlay radio frequency (RF)/multidestinations free-space optical (FSO) links. For RF links, we consider a secondary network with multiple users that can communicate with multiple destinations through a relaying node. The relay is equipped with an antenna array at the RF side, and it uses the amplify-and-forward (AF) protocol. The primary users (PUs) are equipped with multiple antennas at transmit and receive nodes. The RF link is subjected to the aggregate PUs interference effect on the secondary network. To reduce the effect of PUs interference on secondary network at the relay node, two interference cancellation (IC) schemes are adopted, which vary in terms of complexity and achieved performance. On the other hand, the multidestination FSO links can be exploited to further enhance the quality of the second hop, and their associated channel models account for pointing errors, intensity modulation/direct detection, and heterodyne detection. For the aforementioned system model, we obtain exact and asymptotic closed-form expressions for the end-to-end outage probability. To further enhance system performance, optimal power allocation between the two hops is obtained based on the derived asymptotic outage probability expressions.

**Index Terms:** Cognitive radio, multiple-input multiple-output (MIMO), radio frequency (RF), amplify-and-forward (AF) relaying, free-space optical (FSO), interference reduction, spectrum sharing, outage analysis.

## 1. Introduction

Free-space optical (FSO) communications have gained increasing interest due to their advantages, including higher bandwidth and higher capacity, as compared to traditional radio frequency (RF)

wireless communications [1]–[3]. Also, since similar optical transmitters and detectors are used for FSO and fiber optics, similar bandwidth capabilities are achievable. It is also a promising technology as it offers many benefits, including full-duplex Gigabit Ethernet throughput in certain applications, a huge license-free spectrum, a certain immunity to interference, and a high level of security [1], [2]. These benefits of FSO communications can resolve the issues that RF communications face due to the expensive and scarce spectrum.

A part from the promising benefits of FSO communications, these systems are subjected to many real challenges. For instance, the atmospheric turbulence effect may lead to a significant degradation in the performance of FSO systems [1]–[3]. Moreover, thermal expansion, dynamic wind loads, and weak earthquakes result in the building sway phenomenon causing vibration of the transmitter beam thereby leading to a misalignment between FSO transmitter and receiver (also known as pointing errors). It is worthy to learn that intensity modulation/direct detection (IM/DD) is the main mode of detection in FSO systems, but coherent communications have also been proposed as an alternative detection mode. Among these, heterodyne detection is a more complicated detection method, but it can overcome the thermal noise effect (see [4] and references cited therein). In this paper, we consider the effect of pointing errors, as well as the aforementioned detection schemes for the FSO links.

For RF links, cognitive relaying networks (CRNs) are considered as one of the promising solutions for radio spectrum limitations. They can significantly improve the spectral efficiency of wireless networks by intelligently sharing spectrum resources [5]–[7]. A standard approach in spectrum sharing network is the underlay cognitive radio model in which the secondary user (SU) is allowed to share the spectrum with the primary user (PU) simultaneously under an interference limit constraint, which is expected to maintain a reliable communication between PUs nodes. Due to its simplicity, spectrum sharing relay networks with underlay approach has gained much attention in recent years (see [8]–[12] and references therein).

Recently, some research has been devoted toward mixed CRNs and FSO relaying [13], [14]. In [13], the outage performance analysis of a dual-hop relaying system composed of an RF channel cascaded with FSO link was presented. Therein, the RF link was considered as an underlay spectrum sharing network, and FSO link accounted for pointing errors as well as heterodyne and IM/DD techniques. The paper presented the end-to-end signal-to-noise ratio (SNR) outage probability. The work in [13] is extended to [14] by including comprehensive statistical and performance measures. While the preceding works have significantly improved our understanding on the dual-hop relaying with mixed underlay RF and FSO systems, they all assume single-antenna RF system and single FSO link. Also, for RF link, these works assumed that the PU transmitters are located far enough away so as not to impinge any significant interference on the SU relay.

In this paper, we adopt generalized and involved system models as compared to those in [13], [14]. Specifically, we treat multiuser selection in underlay dual-hop mixed RF/FSO relaying where multiple RF users communicate with multiple FSO links through a single AF relay that is equipped with multiple antennas. We consider an RF MIMO configuration that can exploit multi-user diversity and at the same time mitigate the effect of PUs interference at the relay node. In this regard, when the receive antennas at the relay are insufficiently spaced due to space constraints, the use of receive antennas to provide diversity becomes a waste of processing and performance as degraded or no diversity gain becomes feasible. Moreover, to achieve the target of reducing the effect of PUs interference on the secondary network relay, receive interference mitigation schemes become of a great interest to be exploited. Specifically, with the use of sophisticated null-steering techniques, the receive array radiation pattern at the relay can be shaped to place deep nulls in the directions of some *resolvable* PUs interference sources, while providing a maximum array gain in the direction of the desired signal from the served SU transmitter. This interference cancellation can have real applications in RF CRNs as the mitigation of interference on the secondary network is of prime importance when PUs heavily use the spectrum resources. Two interference cancellation algorithms were proposed in [15]–[17], namely dominant receive interference cancellation (DRIC) [15], [16] and adaptive receive interference cancellation (ARIC) [17]. In this paper, we incorporate these two algorithms into the problem formulations for the outage analysis of the mixed underlay

RF MIMO and FSO links and present detailed analytical analysis for both of them to quantify their usefulness and drawbacks in the context of the adopted system models herein.

The main contributions of this work can be summarized as follows:

1) We develop new analytical results of dual-hop AF relaying with mixed underlay RF MIMO and FSO multi-destination network. We consider multiuser selection at the source and the destination for the RF and FSO links, respectively. To mitigate the interference imposed by PUs at the relay, we adopt two ICs algorithms, which are the DRIC and ARIC. The RF links are assumed to follow Rayleigh fading model, whereas the FSO links follow Gamma-Gamma fading model, including the effect of pointing errors. The end-to-end signal-to-interference-plus-noise ratio (SINR) outage probability is obtained in tight closed-form expressions. Also, simple expressions for the end-to-end SINR outage probability at the high SNR are derived and based on that the diversity and coding gains are characterized.

2) We further enhance the end-to-end performance by finding the optimal solutions for the power allocations to minimize the outage probability under constraints of transmit power of secondary transmitters, interference limit on the primary network, and the total end-to-end powers.

3) Our results reveal that under weak atmospheric turbulence conditions, the end-to-end system performance is dominated by RF channel. Hence, the achieved diversity gain depends on the value of the interference power limit $\mathcal{Q}_I$. When $\mathcal{Q}_I$ is proportional to the maximum transmit power $\mathcal{Q}_P$, the achievable diversity gain is $N_S$ for DRIC and ARIC schemes. However, when the interference power limit is fixed, an outage floor appears, hence zero diversity gain for both ICs schemes. In addition, the results indicate that DRIC outperforms ARIC under a deep effect of interference from PUs, but this is obtained with increased complexity and degraded operation efficiency.

4) The FSO channel dominates the achieved results under severe atmospheric turbulence conditions. Therefore, the achievable diversity gain is a result of the minimum value of the turbulence fading and pointing error parameters.

The rest of the paper is organized as follows. The adopted system and channel models are discussed in Section II. Section III addresses the end-to-end outage probability for the two IC algorithms, which are then followed by their respective asymptotic analysis in Section IV. Section V discusses the proposed power allocation approach, and Section VI presents some numerical results that are supported by simulations. Finally, Section VII contains concluding remarks.

*Mathematical Notations:* The notations used herein are as follows. Bold lower/upper case symbols denote vectors/matrices, respectively, $(\cdot)^T$ for transpose, $(\cdot)^H$ for conjugate transpose, and $|\cdot|$ and $\|\cdot\|_F$ are used for the absolute value and the Frobenious norm of vectors/matrices, respectively. The term $f_\beta(x)$ is the PDF of random variable (RV) $\beta$, $F_\beta(x)$ is its CDF, and $\mathcal{R}e\{t\}$ is the real part of a complex quantity $t$. The function $\Gamma(\cdot,\cdot)$ is the upper-incomplete gamma function, which is defined as $\Gamma(z,x) = \int_x^\infty t^{z-1}e^{-t}\mathrm{d}t$, and $\gamma(z,x) = \int_0^x t^{z-1}e^{-t}\mathrm{d}t$ is the lower incomplete gamma function.

## 2. System and Channel Models

We consider a dual hop mixed RF/FSO relay network with multiple RF users. The relay unit $R$ contains multiple receive antennas and an RF receiver on one side, and a photo-aperture transmitter that can potentially serve a specific destination from multiple FSO destinations $D$ on the other side. This implies that the source can communicate with the relay node through RF links, and the relay can transfer data to a specific destination through an FSO link. The relaying system operates in a half-duplex mode over two phases. In the following subsections, we present the signal models of RF and FSO links as shown in Fig. 1.

### 2.1 Signal Model of Underlay Cognitive RF Links

In the first phase, the secondary network contains a total of $N_S$ users and a single relay $R$ that is equipped with $N_R$ antennas. The primary network consists of $L$ PU transmitters $(T_1, \ldots, T_L)$, with
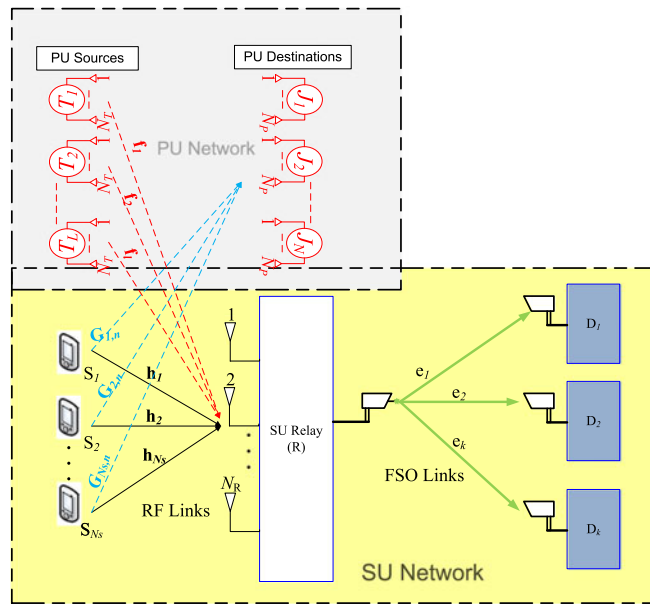
Fig. 1. Adopted system model.

each of which is equipped with $N_T$ antennas, and $N$ PU receivers ($J_1, \ldots, J_N$), where each station is equipped with $N_P$ antennas.

The channel notations adopted can be summarized as follows: the channel gains on the first hop of the secondary network are denoted by $h_{ij}$, for $i \in \{1, \ldots, N_S\}$ and $j \in \{1, \ldots, N_R\}$. Moreover, the channel gains from the $i$th user of the relay node $R$ in the secondary network to the $n$th PU receive station are referred to as $\mathbf{g}_{in} = \{g_{in1}, \ldots, g_{inN_P}\}$ for $i \in \{1, \ldots, N_S\}$ and $n \in \{1, \ldots, N\}$. In addition, the channel gains of interference sources observed from the $L$ PU transmit stations at the $j$th receive antenna of the relay node $R$ are referred to as $\mathbf{f}_{lq} = \{f_{lq1}, \ldots, f_{lqN_R}\}$, for $l \in \{1, \ldots, L\}$ and $q \in \{1, \ldots, N_T\}$. Perfect channel estimation of all associated channel gains are assumed at the secondary network as well as at the PU stations, and they are normalized to have independent and identical complex-valued Gaussian distributions (i.i.d). This assumption can be relaxed but at the expense of more involved analytical treatments.

In this paper, the best user from $N_S$ users is selected (i.e., opportunistic scheduling) to maximize the received SNR at $R$. The receive antennas at $R$ are used to implement an IC scheme to alleviate interference from PUs transmitters. With the use of the time division multiplexing, the SU node $R$ receives a faded signal from its previous source node and $L$ faded interference signals from $L$ PU transmitters. Therefore, the received signal at $R$ is given by

$$\mathbf{y} = \sqrt{P\Omega_h}\mathbf{h}x + \sqrt{P_p \Omega_f} \sum_{l=1}^{L} \mathbf{f}_l \hat{x} + \mathbf{n} \qquad (1)$$

where $P$ is the allocated transmission power at $S$ node, $x$ is the SU transmitted data symbol of normalized power, $P_p$ is the transmission power for all PU transmitters, $\hat{\mathbf{x}}$ is $L \times 1$ PU data symbols vector, $\mathbf{h} = \{h_1, \ldots, h_{N_S}\}$ is $N_S \times 1$ complex channel vector between the $i$-th SU user at $S$ and the $N_R$ receive antennas at $R$, and $\Omega_h$ is the average fading power associated with the desired user at $S$. We further denote $\mathbf{f}_l = \{f_{l1}, \ldots, f_{lN_T}\}$ as the $N_T \times 1$ channel matrix between the $l$-th PU transmitter and the SU $R$ and $\Omega_f$ is the average fading power associated with interfering PU sources. The term $\mathbf{n}$ is $N_S \times 1$ uncorrelated additive white Gaussian noise (AWGN) samples at $S$ where each of which has zero mean and $\sigma^2$ average power. All the transmitted symbols for both PU and SU networks

are with zero mean and unity variance. Transmission interval is assumed to be equal for all time slots.

According to the underlay spectrum sharing model in [5]–[7], the interference power at the $N$ PU receivers originated from the SUs must not exceed a threshold level $I_P$. Therefore, the SUs must transmit with a maximum allowable power at each node that is given by

$$
P = \min\left(P_s, \frac{I_P}{\lambda_g}\right) \tag{2}
$$

where $I_P$ is the PU maximum permissible interference power, $P_s$ is the peak transmission power at all secondary nodes, and $\lambda_g = \|\mathbf{g}_{n*i*}\|^2 = \max_{1 \le n \le N} \|\{g_{i*n}, \ldots, g_{i*n}\}\|^2$ is the largest channel vector from selected $i$-th user at $S$ to the $N$ PU receivers with average fading power $\Omega_g$. To this end, the end-to-end SINR can be expressed as

$$
\gamma_1 = \min\left(\mathcal{Q}_P, \frac{\mathcal{Q}_I}{\lambda_g}\right) \frac{\lambda_h}{1 + \gamma_{1,\text{tot}}} \tag{3}
$$

where $\mathcal{Q}_P = \frac{P_s}{\sigma^2}$, $\mathcal{Q}_I = \frac{I_P}{\sigma^2}$, and $\lambda_h = \max_{1 \le i \le N_S} \|h_{i*}\|^2$ is the SU SNR, and $\gamma_{1,\text{tot}}$ is the residual interference-to-noise ratio (INR) following IC at the relay.

For channel gains that are distributed as i.i.d. complex-valued Gaussian random variables, the distributions for the squares of channel gains, namely $\lambda_g$ and $\lambda_h$, are

*1) The CDF and the PDF of the RV $\lambda_g$ are given by*

$$
F_{\lambda_g}(x) = \left(1 - e^{-\frac{x}{\Omega_g}} \sum_{p=1}^{L_P} \frac{1}{\Gamma(p)} \left(\frac{x}{\Omega_g}\right)^{p-1}\right)^{N_S} \tag{4}
$$

$$
= 1 - \sum_{k_1=1}^{N_S} \binom{N_S}{k_1} (-1)^{k_1 - 1} \Gamma(k_1 + 1)
$$

$$
\times \sum_{|\mathbf{c_p}|=k_1} \mu_p \left(\frac{x}{\Omega_g}\right)^{\lambda_p} \exp\left(-\frac{k_1 x}{\Omega_g}\right) \tag{5}
$$

and

$$
f_{\lambda_g}(x) = \frac{N_S}{\Gamma(L_P)\Omega_g} \sum_{k_4=0}^{N_S-1} \binom{N_S - 1}{k_4} (-1)^{k_4} \Gamma(k_4 + 1)
$$

$$
\times \sum_{|\mathbf{c_n}|=k_4} \mu_n \left(\frac{x}{\Omega_g}\right)^{\lambda_n + L_P - 1} \exp\left(-\frac{(k_4 + 1) x}{\Omega_g}\right) \tag{6}
$$

where $L_P = N N_P$, $\mathbf{c_n} = (c_1, \ldots, c_{N_R}) \in N^{N_R}$ is a multi index $N_R$-tuple vector of nonnegative integers of length $|\mathbf{c_n}| = \sum_{n=1}^{N_R} c_n = k_4$, $\Omega_g$ is the average fading power associated with the desired user, $\mu_n = \frac{1}{\prod_{n=1}^{N_R} \Gamma(c_n+1)\Gamma(n)^{c_n}}$, and $\lambda_n = \sum_{n=1}^{N_R} c_n(n - 1)$.

*Proof:* The derivations of (4) and (6) are obtained by applying the binomial expansion in [29, Eq.1.111] and the power sum expansion of [28, Eq. 9]. ∎

*2) The CDF and the PDF of the RV $\lambda_h$ are given by*

$$
F_{\lambda_h}(x) = \left(1 - \exp\left(-\frac{x}{\Omega_g}\right)\right)^{N_S}
$$

$$
= \sum_{k_1=0}^{N_S} \binom{N_S}{k_1} (-1)^{k_1} \exp\left(-\frac{k_1 x}{\Omega_h}\right) \tag{7}
$$

and

$$f_{\lambda_h}(x) = \frac{N_S}{\Omega_h} \sum_{k_1=0}^{N_S-1} \binom{N_S - 1}{k_1}(-1)^{k_1} \exp\left(-\frac{(k_1+1)x}{\Omega_h}\right). \tag{8}$$

### 2.2 Receive IC Schemes

This part outlines the two receive IC schemes at the relay. Moreover, it briefly presents the statistics of the residual INR, $\gamma_{l,\text{tot}}$.

*2.2.1) DRIC Scheme:* This technique requires the discrimination of different PUs interference powers and then ordering them according to their levels. Apparently, the associated processing increases the complexity of shaping the receive array pattern. Moreover, the effect of imprecise ordering of PUs interference power levels has to be addressed. It will be shown in the sequel that statistical ordering imperfectness can diminish the expected performance advantage from accurately eliminating the most dominant set of PUs interfering signals. Then the best scenario is to eliminate as many of arbitrarily chosen PUs interfering signals, according to the size of the operating receive array at the relay node.

Now, we define $|\gamma_{(1),l}|^2 < |\gamma_{(2),l}|^2 < \ldots < |\gamma_{(L),l}|^2$ as the order statistics obtained by arranging $\{|\gamma_{l,l}|^2\}_{l=1}^L$ in an increasing order of magnitude and we assume that the receiver attempts to eliminate the most effective $N_R - 1$ interfering powers. Then, the total residual INR becomes $\gamma_{l,\text{tot}} = \overline{\gamma}_l \sum_{l=1}^{L_A} ||\gamma_{(l),l}|^2$, where $L_A = L_T - (N_R - 1)$.

The term $L_A$ represents the residual number of PUs interfering signals when the receive array at $R$ operates to eliminate the most dominant $N_R - 1$ interfering powers. For the case of overloaded receive array (i.e., $L_T > N_R - 1$), $L_A$ is always greater than zero. On the other hand, for the case of under-loaded receive array (i.e., $L_T \leq N_R - 1$), $L_A$ can be as small as zero. However, when a limited number of receive antennas can be turned on at a specific time, $L_A$ increases linearly with the decrease in the number of active antennas. The limiting case OF $N_R = 1$ is the scenario of no IC.

Considering the impact of outdated order statistics with $\tau$ being the excess time delay indicator, and according to [15], [20], the distribution of $\gamma_{l,\text{tot}}$ can be expressed as

$$f_{\gamma_{l,\text{tot}|0\leq\tau<+\infty}}(x) = \frac{1}{\overline{\gamma}_l}\binom{L_T}{L_A} \sum_{g=0}^{L_A-1} (-1)^g \binom{L_A}{g} \beta_1(\rho_l)$$

$$\times \left(\frac{L_A - g}{N_R - 1}\right)^{L_A-1} \exp\left(\frac{-x(\beta_2(\rho_l)\cdot(L_T - g))}{(\overline{\gamma}_l(L_A - g))}\right); x \geq 0 \tag{9}$$

where $\beta_1(\rho_l) \triangleq (\rho_l^2)^{1-L_A}(1 + \frac{(1-\rho_l^2)(N_R-1)}{L_A-g})^{L_A-2}$, $\beta_2(\rho_l) \triangleq (1 + \frac{(1-\rho_l^2)(N_R-1)}{L_A-g})^{-1}$, and $\rho_l$ is the envelope correlation coefficient of the underlying complex-valued Gaussian fading process, which is related to the value of $\tau$. For instance, the Clark's model suggests that $\rho_l = |J_0(2\pi\Delta f_m \tau)|$, where $J_0(x)$ is the Bessel function of the first kind with zero-order and $\Delta f_m$ is the maximum Doppler spread.

Note that the best case from the desired user point of view takes place when $\tau = 0$, whereas the statistical order of interferer's powers becomes useless when $\tau \to +\infty$. In this case, the best receive antenna array can eliminate a total of $N_R - 1$ arbitrarily chosen interfering signals. The distribution of $\gamma_{k,l,\text{tot}}$, in this case, can be explicitly written as

$$f_{\gamma_{k,l,\text{tot}|\tau\to+\infty}}(x) = \frac{1}{\Gamma(L_A)}\left(\frac{1}{\overline{\gamma}_{k,l}}\right)^{L_A} x^{L_A-1} e^{-x/\overline{\gamma}_{k,l}}; x \geq 0. \tag{10}$$

*2.2.2) ARIC Scheme:* Different from the technique described in the preceding part, the ARIC does not require predicting and ordering the interference power levels, and therefore, it is relatively less complex. In addition, this prediction and ordering may return marginal benefits, particularly when these estimates are outdated or when the number of strong interferer's is relatively large. The ARIC considers the case when the size of the receive array is adaptively varied according to

the experienced level of interference. Specifically, the possible occasions of low interference effect can be captured and reflected into reducing the receive IC processing at the relay. On the other hand, the operation at full receive array capacity is only needed when the PUs interference effect is significant.

The IC scheme herein aims to reduce the number of active receive antennas by adaptively activating as many antennas as necessary to have the total residual INR below a specific threshold, $\gamma_{I,T}$. The resulting residual INR can be written as $\gamma_{I,\text{tot}} = \sum_{l=1}^{L_A} \gamma_{I,l}$, where $L_A = L_T - (N_R - 1)$ is the remaining number of interfering signals. According to the results in [16], the distribution of $\gamma_{k,I,\text{tot}}$ in this case can be expressed as

$$
f_{\gamma_{I,\text{tot}}}(x) = \frac{1}{\Gamma(L_A)} \left(\frac{1}{\bar{\gamma}_I}\right)^{L_A} x^{L_A - 1} e^{-x/\bar{\gamma}_{k,I}} U(x - \gamma_{I,T})
$$

$$
+ \left(\frac{1}{\Gamma(L_T)} \left(\frac{1}{\bar{\gamma}_I}\right)^{L_T} x^{L_T - 1} e^{-x/\bar{\gamma}_I} + e^{-\gamma_{I,T}/\bar{\gamma}_I}\right)
$$

$$
\times \sum_{h=2}^{L_R} \frac{\left(\frac{1}{\bar{\gamma}_I}\right)^{\iota}}{\Gamma(\iota)} x^{\iota-1}\right) \left(U(x) - U(x - \gamma_{I,T})\right) \tag{11}
$$

where $\iota = L_T - (h - 1)$. The case when all receive antennas are active intuitively implies that the residual INR will be above $\gamma_{I,T}$, and the distribution of $\gamma_{I,\text{tot}}$, in this case, follows a similar form to that shown in (10). On the other hand, when the residual INR is below $\gamma_{I,T}$, the active number of receive antennas becomes variable and takes on values from the set $\{1, 2, \ldots, L_R\}$ with different probabilities. Therefore, the distribution $\gamma_{I,\text{tot}}$ counts for the effect of the PUs interference power distributions and the randomness in the number of active receive antennas at $R$.

Note that (9) and (11), when $L_R = 1$ (i.e., no cancelation), reduce to a form that is similar to (10) with $L_A$ therein replaced by $L_T$. The interference-free scenario with $\gamma_{k,I,\text{tot}} = 0$ in (9)–(11) can be reached only in under-loaded case, for which $L_T \leq N_R - 1$, and $\gamma_{I,T} \to 0$ in (11), with $L_A = 0$.

### 2.3 Signal Model of FSO Links

In the second phase, we assume $R$ is equipped with single transmit aperture, and there are $N_D$ SU destinations where each of which is equipped with single receive aperture. The information bits are modulated via a coherent detection technique or an IM/DD technique. A high-energy FSO system is assumed wherein the performance is obstructed by the background radiation and the thermal noise. Under this assumption, the AWGN model is an appropriate approximation for the Poisson photon counting detection model [22]. Hence, the channel notation adopted in the second hop is $\mathbf{e}$ that denotes the $N_D \times 1$ channel vector for the $R \to D$ link with channel coefficients $e_k$, for $k \in \{1, \ldots, N_D\}$. It must be noted that the random variables in $\mathbf{e}$ are assumed to follow i.i.d. random variable (Gamma-Gamma) distributions. This assumption is justified for link distances falling in the order of kilometers along with the aperture separation distances being in the order of centimeters [23]. Now, at the relay, the best destination is selected to maximize the received SNR at $D$. Therefore, the received signal at the $j$th selected $D$ is given as

$$
z = \eta\, e_j\, y + n_2 \tag{12}
$$

where $\eta$ is the optical-to-electrical conversion coefficient, $e_j$ complex channel vector between the transmit aperture at $R$ and the $j$th selected $D$, and the term $n_2$ represents an uncorrelated AWGN sample at $D$ having zero mean and $\sigma^2$ average power. To this end, the instantaneous SNR for the second (i.e. $R \to D$) hop is expressed as

$$
\gamma_2 = \eta^2 \lambda_e \tag{13}
$$

where $\lambda_e = \|e_j\|^2 = \max_{1 \le k \le N_D} \|e_k\|^2$ is the instantaneous SNR of the second (i.e. $R \to D$) hop. It is important to note that $e_j = e_{j_a} e_{j_p}$, where $e_{j_a}$ is the irradiance for the atmospheric turbulence and $e_{j_p}$ is the irradiance for the pointing errors.

With the assumption that the atmospheric turbulence conditions of the FSO channels are distributed as i.i.d. Gamma-Gamma along with being effected by the pointing errors, we present the following distributions for the squares of channel amplitudes of $\lambda_e$ as:

*1) The CDF and PDF of the RV $\lambda_e$ are given respectively by [4]*

$$F_{\lambda_e}(\gamma_2) = \left( A \, G_{r+1,3r+1}^{3r,1} \left[ \frac{B}{C_r \, \overline{\gamma}_2} \gamma_2 \, \middle| \, \begin{matrix} 1, \kappa_1 \\ \kappa_2, 0 \end{matrix} \right] \right)^{N_D} \tag{14}$$

$$f_{\lambda_e}(\gamma_2) = \frac{N_D}{\gamma_2} \left[ \frac{r^{\alpha+\beta-2} \, \xi^2}{(2\,\pi)^{r-1} \, \Gamma(\alpha) \, \Gamma(\beta)} \right]^{N_D}$$

$$\times \, G_{r,3r}^{3r,0} \left[ \left( \frac{\alpha\beta}{r^2} \right)^r \frac{\gamma_2}{C_r \, \overline{\gamma}_2} \, \middle| \, \begin{matrix} \kappa_1 \\ \kappa_2 \end{matrix} \right]$$

$$\times \left( G_{r+1,3r+1}^{3r,1} \left[ \left( \frac{\alpha\beta}{r^2} \right)^r \frac{\gamma_2}{C_r \, \overline{\gamma}_2} \, \middle| \, \begin{matrix} 1, \kappa_1 \\ \kappa_2, 0 \end{matrix} \right] \right)^{N_D-1} \tag{15}$$

where $A = \frac{r^{\alpha+\beta-2} \, \xi^2}{(2\pi)^{r-1} \Gamma(\alpha) \Gamma(\beta)}$, $B = \frac{(\xi^2 \alpha \beta)^r}{(\xi^2+1)^r r^{2r}}$, $\kappa_1 = \frac{\xi^2+1}{r}, \ldots, \frac{\xi^2+r}{r}$ comprises of $r$ terms, $\kappa_2 = \frac{\xi^2}{r}, \ldots,$

$\frac{\xi^2+r-1}{r}, \frac{\alpha}{r}, \ldots, \frac{\alpha+r-1}{r}, \frac{\beta}{r}, \ldots, \frac{\beta+r-1}{r}$ comprises of $3r$ terms, $r$ is the parameter defining the type of detection technique (i.e., $r = 1$ represents heterodyne detection and $r = 2$ represents IM/DD), $\alpha$ and $\beta$ are the fading/scintillation parameters related to the atmospheric turbulence conditions, $\xi$ is the ratio between the equivalent beam radius at the receiver and the pointing error displacement standard deviation (jitter) at the receiver [25], $C_1 = 1$ and $C_2 = \alpha \beta \, (\xi^2 + 1) \, (\xi^2 + 2) / [(\alpha + 1) \, (\beta + 1) \, \xi^4]$, $\overline{\gamma}_2$ is the average SNR of the second (i.e. $R \to D$) hop, $\Gamma(.)$ is the Gamma function as defined in [29, Eq. (8.310)], and $G[.]$ is the Meijer's G function as defined in [29, Eq. (9.301)].

## 3. End-to-End Outage Probability Analysis

In this section, we investigate the outage probability of multiuser mixed RF/multi-destinations FSO links in underlay cognitive relay network. Specifically, we derive the new analytical expressions for the exact end-to-end outage probability of the proposed system model for two different interference cancellation schemes namely DRIC and ARIC.

The outage probability is *defined* as an important performance indicator of wireless communication systems, which is defined as the probability that the instantaneous end-to-end SINR falls below a given threshold $P_{out} = \Pr\left[\gamma_{up} \le \gamma_{th}\right]$. Hence, the outage probability can be written as

$$P_{out}(\gamma_{th}) = F_{\gamma_{1,(\chi)}}(\gamma_{th}) + F_{\gamma_2}(\gamma_{th}) - F_{\gamma_{1,(\chi)}}(\gamma_{th}) F_{\gamma_2}(\gamma_{th}) \tag{16}$$

where $\chi = \{$DRIC, ARIC$\}$. Next, in the following two subsections, we present the end-to-end outage probability for DRIC and ARIC schemes.

### 3.1 Dominant Interference Cancellation

To find the end-to-end outage probability, we need first to evaluate $F_{\gamma_{1,DRIC}}(\gamma)$ and $F_{\gamma_2}(\gamma_{th})$. For FSO link, the CDF of $\gamma_2$ is given by (14). For the underlay RF-link, we present a new compact closed-form expression of $F_{\gamma_{1,DRIC}}(\gamma)$ in the following key result.

*Lemma 1. The CDF of RV $\gamma_{1,\text{DRIC}}$ for the underly RF link is given by*

$$F_{\gamma_{1,\text{DRIC}}}(\gamma_{\text{th}}) = F_{\lambda_g}\left(\frac{\mathcal{Q}_I}{\mathcal{Q}_P}\right)\left(1 - \frac{1}{\bar{\gamma}_1}\binom{L_T}{L_A}\sum_{g=0}^{L_A-1}\binom{L_A}{g}(-1)^g\beta_1(\rho_I)\left(\frac{L_A - g}{L_T - L_A}\right)^{L_A-1}\sum_{k_1=0}^{N_S}\binom{N_S}{k_1}(-1)^{k_1}\right.$$

$$\times \exp\left(\frac{-k_1\gamma_{\text{th}}}{\Omega_h\mathcal{Q}_P}\right)\left(\frac{\beta_2(\rho_I)(L_T - g)}{\bar{\gamma}_{k,I}(L_A - g)} + \frac{k_1\gamma_{\text{th}}}{\Omega_h\mathcal{Q}_P}\right)^{-1}\right) + \left(1 - F_{\lambda_g}\left(\frac{\mathcal{Q}_I}{\mathcal{Q}_P}\right)\right)$$

$$- \frac{L_T}{\Gamma(N)\bar{\gamma}_g}\sum_{k_1=0}^{N_S}\binom{N_S}{k_1}(-1)^{k_1}\sum_{k_3=0}^{L_T-1}\binom{L-1}{k_3}(-1)^{k_3}\Gamma(k_3 + 1)\sum_{|\mathbf{c}_I|=k_3}\mu_I\left(\frac{1}{\Omega_g}\right)^{\lambda_I+N-1}$$

$$\times \exp\left(-\frac{\mathcal{Q}_I}{Q_P}\phi\right)\sum_{k=0}^{\mu_2-1}\frac{\Gamma(\mu_2)}{\Gamma(k+1)}\left(\frac{\mathcal{Q}_I}{\mathcal{Q}_P}\right)^k\left(\frac{1}{\phi}\right)^{a_1}\frac{1}{\bar{\gamma}_1}\binom{L_T}{L_A}\sum_{g=0}^{L_A-1}\binom{L_A}{g}(-1)^g\beta_1(\rho_I)$$

$$\times \left(\frac{L_A - g}{L_T - L_A}\right)^{L_A-1}\frac{1}{\alpha}\left(\frac{\alpha\phi\mathcal{Q}_I\Omega_h}{k_1\gamma_{\text{th}}}\right)^{\frac{a_1}{2}}\exp\left(\frac{\alpha\phi\mathcal{Q}_I\Omega_h}{2k_1\gamma_{\text{th}}}\right)W_{-\frac{a_1}{2}, \frac{1-a_1}{2}}\left(\frac{\alpha\phi\mathcal{Q}_I\Omega_h}{k_1\gamma_{\text{th}}}\right) \quad (17)$$

where $\phi = \frac{k_1\gamma_{\text{th}}}{\bar{\gamma}_{hQ_I}} + \frac{k_3+1}{\bar{\gamma}_g}$ , $a_1 = \lambda_2 - k$, $\alpha = \left(\frac{\beta_2(\rho_I(L_T-g))}{\bar{\gamma}_{k,I}(L_T-g)} + \frac{\mathcal{Q}_I k_1}{\mathcal{Q}_P}\right)$, and $W_{a,b}(.)$ is the Whittaker function [29, 9.220.4].
Proof: See Appendix A                                                                            ∎

Note that our result in Lemma (1) involves standard functions and only special Whittaker function which allows for fast evaluation in popular mathematical software such as Matlab, thereby providing an efficient means to evaluate the outage probability and avoiding the time-consuming Monte Carlo simulations.

### 3.2 Adaptive Interference Cancellation

For adaptive interference cancellation scheme, we find the following key result for CDF of RF link in Lemma 2.

*Lemma 2: The CDF of RV $\gamma_{1,\text{ARIC}}$ for the underly RF link is given by*

$$F_{\gamma_{1,\text{ARIC}}}(\gamma_{\text{th}}) = \sum_{k_1=0}^{N_S}\binom{N_S}{k_1}(-1)^{k_1}\exp\left(-\frac{k_1\gamma_{\text{th}}}{\Omega_h Q_P}\right)\left[\frac{1}{\Gamma(L_A)}\left(\frac{1}{\bar{\gamma}_1}\right)^{L_A}\Gamma\left(L_A, \gamma_{1,T}\zeta_1\right)\zeta_1^{-L_A} + \frac{1}{\Gamma(L)}\left(\frac{1}{\bar{\gamma}_1}\right)^L\right.$$

$$\times \gamma\left(L_T, \gamma_{1,T}\zeta_1\right)\zeta_1^{-L_T} + e^{-\gamma_{1,T}/\bar{\gamma}_1}\sum_{h=2}^{N_R}\left(\frac{1}{\bar{\gamma}_1}\right)^{L-(h-1)}\frac{1}{\Gamma(L_T-(h-1))}\gamma\left(L_T - h + 1, \gamma_{1,T}\zeta_1\right)\zeta_1^{h-L_T-1}\right]$$

$$\times \frac{L_T}{\Gamma(N)\Omega_g}\sum_{k_1=0}^{N_S}\binom{N_S}{k_1}(-1)^{k_1}\sum_{k_3=0}^{L_T-1}\binom{L_T-1}{k_3}(-1)^{k_3}\Gamma(k_3 + 1)\sum_{|\mathbf{c}_I|=k_3}\mu_I\left(\frac{1}{\Omega_g}\right)^{b_1}\sum_{k=0}^{\mu_2-1}\frac{\Gamma(\mu_2)}{\Gamma(k+1)}\left(\frac{Q_I}{Q_P}\right)^k$$

$$\times \exp\left(-\frac{Q_I}{Q_P}\phi\right)\left(\frac{1}{\phi}\right)^{\mu_2-k}\times\left[\frac{1}{\Gamma(L_A)}\left(\frac{1}{\bar{\gamma}_1}\right)^{L_A}\sum_{g_1=0}^{L_A-1}\binom{L_A-1}{g_1}(-1)^{g_1}\varpi^{\frac{b_2}{2}-1}\left(\frac{\phi}{k_1\theta}\right)^{L_A+\frac{b_2}{2}-1}\right.$$

$$\times \chi^{-\frac{b_2}{2}}\exp\left(\frac{-\varpi}{2}\delta\right)W_{-\frac{b_2}{2}, \frac{1-b_2}{2}}(\varpi\delta) + \frac{1}{\Gamma(L_T)}\left(\frac{1}{\bar{\gamma}_1}\right)^{L_T}\sum_{g_2=0}^{L_T-1}\binom{L_T-1}{g_2}(-1)^{g_2}\varpi^{\frac{a_3}{2}-1}\left(\frac{\phi}{k_1\theta}\right)^{L_T+\frac{b_3}{2}-1}$$

$$\times \exp\left(\frac{\varpi\phi}{2k_1\theta}\right)\left(W_{-\frac{b_3}{2},\frac{1-b_3}{2}}\left(\frac{\varpi\phi}{k_1\theta}\right) - \chi^{-\frac{b_3}{2}}\exp\left(-\frac{\varpi\gamma_{l,T}}{2}\right)W_{-\frac{b_3}{2},\frac{1-b_3}{2}}(\zeta_1)\right) + \sum_{h=2}^{N_R}\frac{\exp-\frac{\gamma_{l,T}}{\bar{\gamma}_l}\left(\frac{1}{\bar{\gamma}_l}\right)^{b_5}}{\Gamma(b_5)}$$

$$\times \sum_{g_3=0}^{L_T-h}\binom{L_T-h}{g_3}(-1)^{g_3}\frac{\exp\left(\frac{\varpi_2\phi}{2k_1\theta}\right)}{\varpi_2^{-\frac{b_4}{2}+1}\left(\frac{\phi}{k_1\theta}\right)^{-L_T+h-\frac{b_4}{2}}}\left(W_{-\frac{a_4}{2},\frac{1-a_4}{2}}\left(\frac{\varpi_2\phi}{k_1\theta}\right) - \frac{\exp\left(-\frac{\varpi_2\gamma_{l,T}}{2}\right)}{\chi^{\frac{a_4}{2}}}W_{-\frac{b_4}{2},\frac{1-b_4}{2}}(\varpi_2\delta)\right)\Bigg]$$

$$(18)$$

where $\varpi = \frac{Q_l k_1\theta}{Q_P} + \frac{1}{\bar{\gamma}_l}$, $\varpi_2 = \frac{Q_l k_1\theta}{Q_P}$, $b_2 = -(L_A - g_1 - \mu 2 + k - 1)$, $b_3 = -(L_T - g_2 - \mu 2 + k - 1)$, $b_4 = -(L_T - h - g_3 - \mu 2 + k)$, $b_5 = L - (h - 1)$ $\chi = (1 + \gamma_{l,T}\frac{k_1\theta}{\phi})$, $\delta = (\frac{\phi}{k_1\theta} + \gamma_{l,T})$, and $\zeta_1 = \left(\frac{k_1\gamma_{th}}{\Omega_h Q_P} + \frac{1}{\bar{\gamma}_l}\right)$.

*Proof:* See Appendix B. ∎

## 4. End-to-End Asymptotic Outage Probability Analysis

In this section, we derive the outage probability in the asymptotic regime based on which the diversity and coding gains achieved by the system are investigated. Without loss of generality, we assume two practical scenarios for the RF link: I) proportional interference power constraint where the peak interference power is proportional to the maximum transmit power such that $Q_l = \mu Q_P$ when $Q_P \to \infty$, where $\mu$ is a positive constant and II) fixed interference power constraint where the peak interference power is fixed and independent of the maximum transmit as $Q_P \to \infty$. Therefore, the end-to-end outage probability in the high SNR is given by

$$P_{\text{out}}^\infty(\gamma_{\text{th}}) \approx F_{\gamma_{1.(\chi)}}^\infty(\gamma_{\text{th}}) + F_{\gamma_2}^\infty(\gamma_{\text{th}}),\tag{19}$$

where $F_{\gamma_{1.(\chi)}}^\infty(\gamma_{\text{th}})$ and $F_{\gamma_2}^\infty(\gamma_{\text{th}})$ are the approximated CDFs in the high SNR of RF and FSO links, respectively. For FSO links, the CDF of $\gamma_2$ can be approximated in the high SNR $\bar{\gamma}_2 \to \infty$. Utilizing (14) and applying [4, App., Eq. (41)], the CDF for the Gamma-Gamma model in (14) can be given asymptotically, at **high SNR**, in a simpler form in terms of basic elementary functions as

$$F_{\gamma_2}(\gamma_{\text{th}})\underset{\mu_r>>1}{\cong}\left[A\sum_{k=1}^{3r}\left(\frac{C_r\bar{\gamma}_2}{B\gamma_{\text{th}}}\right)^{-\kappa_{2,k}}\right.$$

$$\left.\times\frac{\prod_{l=1;l\neq k}^{3r}\Gamma(\kappa_{2,l}-\kappa_{2,k})}{\kappa_{2,k}\prod_{l=2}^{r+1}\Gamma(\kappa_{1,l}-\kappa_{2,k})}\right]^{N_D\frac{\vartheta}{r}}\tag{20}$$

where $\kappa_{u,v}$ represents the $v^{\text{th}}$-term of $\kappa_u$. The asymptotic expression for the CDF in (20) is dominated by the min($\xi, \alpha, \beta$) where $\xi$ represents the 1$^{\text{st}}$-term, $\alpha$ represents the $(r+1)^{\text{th}}$-term, and $\beta$ represents the $(2r+1)^{\text{th}}$-term in $\kappa_2$ i.e. when the difference between the parameters is greater than 1 then the asymptotic expression for the CDF in (20) is dominated by a single term that has the least value among the above three parameters i.e. $\xi$, $\alpha$, and $\beta$. On the other hand, if the difference between any two parameters is less than 1 then the asymptotic expression for the CDF in (20) is dominated by the summation of the two terms that have the least value among the above three parameters with a difference less than 1 and so on and so forth. Therefore, based on a single dominant term, the asymptotic expression can be written as

$$F_{\gamma_2}^\infty(\gamma_{\text{th}}) \approx \Pi\left(\frac{\gamma_{\text{th}}}{\bar{\gamma}_2}\right)^{N_D\frac{\vartheta}{r}}\tag{21}$$

where

$$\Pi = \left[ A \left( \frac{C_r}{B} \right)^{-\vartheta} \frac{\prod_{l=1; \kappa_{2,l} \neq \vartheta}^{3r} \Gamma(\kappa_{2,l} - \vartheta)}{\vartheta \prod_{l=2}^{r+1} \Gamma(\kappa_{1,l} - \vartheta)} \right]^{N_D \frac{\vartheta}{r}} \tag{22}$$

and $\vartheta = \min(\xi^2, \alpha, \beta)$.

For the RF link, we present the asymptotic CDF for the two cancellation scenarios in the following subsections.

### 4.1 Dominant Interference Cancellation

1) *Proportional interference power constraint*: This scenario assumes the PU receiver is able to tolerate a large amount of interference from SU users. Hence, we present the following key result.

*Lemma 3. The asymptotic CDF of the underlay RF link is given by*

$$F_{\gamma_{1,\text{DRIC}}}^{\infty}(\gamma_{\text{th}}) \approx \Xi \left( \frac{\gamma_{\text{th}}}{\mathcal{Q}_P} \right)^{N_S} \tag{23}$$

where $\Xi$ is

$$\Xi = \frac{1}{\bar{\gamma}_1} \left( \frac{\gamma_{\text{th}}}{\bar{\gamma}_h} \right)^{N_S} \binom{L}{L_A} \sum_{g=0}^{L_A - 1} \binom{L_A}{g} (-1)^g \beta_1(\rho_l) \left( \frac{L_A - g}{L - L_A} \right)^{L_A - 1} \sum_{j=0}^{N_S} \binom{N_S}{j} \Gamma(j + 1)$$

$$\times \left( \frac{\beta_2(\rho_l)(L - g)}{\bar{\gamma}_l(L_A - g)} \right)^{-j-1} \left( \mathcal{Q}_P^{N_S} F_{\gamma_{k,h}} \left( \frac{Q_l}{Q_P} \right) + \left( \frac{\bar{\gamma}_g}{Q_l} \right)^{N_S} \frac{L}{\Gamma(N)} \sum_{k_3=0}^{L-1} \binom{L-1}{k_3} (-1)^{k_3} \right.$$

$$\left. \times \Gamma(k_3 + 1) \sum_{|\mathbf{c}_l| = k_3} \mu_l \frac{\Gamma\left( N_S + \lambda_l + N, \frac{Q_l(k_3 + 1)}{Q_P \bar{\gamma}_g} \right)}{(k_3 + 1)^{(N_S + \lambda_l + N)}} \right). \tag{24}$$

*Proof:* By utilizing the Maclaurin series expansion of the exponential function and neglecting the higher order function of the CDF of $\lambda_h$, and then repeating the same procedure as adopted in Appendix A, the final result is obtained. ∎

Hence, the end-to-end asymptotic outage probability of mixed underlay RF/FSO network with DRIC model when $\bar{\gamma} = \mathcal{Q}_P = \bar{\gamma}_2$ as $\bar{\gamma} \to \infty$ is given by

$$P_{\text{out}}^{\infty}(\gamma_{\text{th}}) = \begin{cases} \Xi \left( \frac{\gamma_{\text{th}}}{\bar{\gamma}} \right)^{N_S}, & \text{if} \quad N_S < N_D \frac{\vartheta}{r} \\ \Pi \left( \frac{\gamma_{\text{th}}}{\bar{\gamma}} \right)^{N_D \frac{\vartheta}{r}}, & \text{if} \quad N_S > N_D \frac{\vartheta}{r} \\ (\Xi + \Pi) \left( \frac{\gamma_{\text{th}}}{\bar{\gamma}} \right)^{\mathcal{N}}, & \text{if} \quad \mathcal{N} = N_S = N_D \frac{\vartheta}{r}. \end{cases} \tag{25}$$

2) *Fixed interference power constraint*: This scenario considers $\mathcal{Q}_l$ is fixed and $\mathcal{Q}_P$ grows large in the high SNR. Hence, we present the following key result.

*Lemma 4. The asymptotic CDF of RF link is given by*

$$F_{\gamma_{1,\text{DRIC}}}^{\infty}(\gamma_{\text{th}}) \approx \left( \Delta_1 \left( \frac{1}{\mathcal{Q}_P} \right)^{N_S} + \Delta_2 \left( \frac{1}{\mathcal{Q}_l} \right)^{N_S} \right) \gamma_{\text{th}}^{N_S} \tag{26}$$

where $\Delta_1$ and $\Delta_2$ are given, respectively, by

$$
\begin{aligned}
\Delta_1 = \frac{1}{\overline{\gamma}_l}\binom{L_T}{L_A} \sum_{g=0}^{L_A-1}(-1)^g\binom{L_A}{g}\beta_1(\rho_l)\left(\frac{L_A-g}{N_R-1}\right)^{L_A-1}\exp\left(\frac{\beta_2(\rho_l)\cdot(L_T-g)}{\overline{\gamma}_l(L_A-g)}\right) \\
\times\left(\frac{\beta_2(\rho_l)\cdot(L_T-g)}{\overline{\gamma}_l(L_A-g)}\right)^{-(N_S+1)}\Gamma\left(N_S+1,\frac{\beta_2(\rho_l)\cdot(L_T-g)}{\overline{\gamma}_l(L_A-g)}\right)F_{\lambda_g}\left(\frac{\mathcal{Q}_l}{\mathcal{Q}_P}\right)
\end{aligned}
\tag{27}
$$

$$
\begin{aligned}
\Delta_2 = \frac{1}{\overline{\gamma}_l}\binom{L_T}{L_A}\sum_{g=0}^{L_A-1}(-1)^g\binom{L_A}{g}\beta_1(\rho_l)\left(\frac{L_A-g}{N_R-1}\right)^{L_A-1}\exp\left(\frac{\beta_2(\rho_l)\cdot(L_T-g)}{\overline{\gamma}_l(L_A-g)}\right)\left(\frac{\beta_2(\rho_l)\cdot(L_T-g)}{\overline{\gamma}_l(L_A-g)}\right)^{-(N_S+1)} \\
\times\Gamma\left(N_S+1,\frac{\beta_2(\rho_l)\cdot(L_T-g)}{\overline{\gamma}_l(L_A-g)}\right)\frac{N_S}{\Gamma(N)}\mu^{-N_S}s\sum_{r=0}^{N_S-1}N_{S-1} \\
\times C_r\sum_{r_p:N}\frac{1}{\psi(r_n)}\left(\Omega_g\right)^{N_S-1}(r+1)^{-a_3}\Gamma\left(a_3,\frac{(r+1)\mathcal{Q}_l}{\Omega_g\mathcal{Q}_P}\right).
\end{aligned}
\tag{28}
$$

*Proof:* Follow the same proof as adopted in Lemma 2.  ■

For fixed interference power constraint, we obtain the end-to-end asymptotic outage probability of mixed underlay RF/FSO network as follows:

$$
P_{\text{out}}^\infty(\gamma_{\text{th}}) = \begin{cases} \left(\frac{\Delta_1}{\overline{\gamma}^{N_S}}+\frac{\Delta_2}{\mathcal{Q}_l^{N_S}}\right)\gamma_{\text{th}}^{N_S}, & \text{if} \quad N_S < N_D\frac{\vartheta}{r} \\ \Pi\left(\frac{\gamma_{\text{th}}}{\overline{\gamma}}\right)^{N_D\frac{\vartheta}{r}}, & \text{if} \quad N_S > N_D\frac{\vartheta}{r} \\ \left(\frac{\Delta_1+\Pi}{\overline{\gamma}^{\mathcal{N}}}+\frac{\Delta_2}{\mathcal{Q}_l^{\mathcal{N}}}\right)\gamma_{\text{th}}^{\mathcal{N}}, & \text{if} \quad \mathcal{N}=N_S=N_D\frac{\vartheta}{r}. \end{cases}
\tag{29}
$$

### 4.2 Adaptive Interference Cancellation

In this subsection, we derive the end-to-end asymptotic outage probability for the adaptive interference cancellation scheme. To proceed further, we only need to derive the asymptotic CDF of the first link $F_{\gamma_{1,\text{ARIC}}}(\gamma_{\text{th}})$.

1) *Proportional interference power constraint:* For adaptive interference cancellation we have the following result.

*Lemma 5:* The asymptotic CDF of cognitive underlay RF link is given by

$$
F_{\gamma_{1,\text{ARIC}}}^\infty(\gamma_{\text{th}}) \approx \Theta\left(\frac{\gamma_{\text{th}}}{\mathcal{Q}_P}\right)^{N_S}
\tag{30}
$$

where $\Theta$ is $b_6 = L + j - h + 1$.

$$
\begin{aligned}
\Theta = \sum_{j=0}^{N_S}\binom{N_S}{j}\left[\frac{\overline{\gamma}_l^j}{\Gamma(L_A)}\Gamma\left(L_A+j,\frac{\gamma_{1,T}}{\overline{\gamma}_l}\right)+\frac{\overline{\gamma}_l^j}{\Gamma(L_T)}\gamma\left(L_T+j,\frac{\gamma_{1,T}}{\overline{\gamma}_l}\right)+e^{-\gamma_{1,T}/\overline{\gamma}_l}\sum_{h=2}^{N_R}\left(\frac{1}{\overline{\gamma}_l}\right)^{b_5}\frac{\gamma_{1,T}^{b_6}}{(b_6)\Gamma(b_5)}\right] \\
\left(Q_P^{N_S}F_{\gamma_g}(\mu)+\left(\frac{\Omega_{k,g}}{Q_l}\right)^{N_S}\frac{L_T}{\Gamma(N)}\sum_{k_3=0}^{L_T-1}\binom{L_T-1}{k_3}(-1)^{k_3}\Gamma(k_3+1)\sum_{|\mathbf{c}_l|=k_3}\mu_l\frac{\Gamma\left(N_S+\lambda_l+N,\frac{Q_l(k_3+1)}{Q_P\Omega_{k,g}}\right)}{(k_3+1)^{(N_S+\lambda_l+N)}}\right).
\end{aligned}
\tag{31}
$$

*Proof:* In the following, we obtain the end-to-end asymptotic outage probability of mixed underlay RF/FSO network when $\bar{\gamma} = \mathcal{Q}_P = \bar{\gamma}_2$ as $\bar{\gamma} \to \infty$ is given by

$$P_{\text{out}}^{\infty}(\gamma_{\text{th}}) = \begin{cases} \Theta\left(\frac{\gamma_{\text{th}}}{\bar{\gamma}}\right)^{N_S}, & \text{if} \quad N_S < N_D\frac{\vartheta}{r} \\ \Pi\left(\frac{\gamma_{\text{th}}}{\bar{\gamma}}\right)^{N_D}, & \text{if} \quad N_S > N_D\frac{\vartheta}{r} \\ (\Theta + \Pi)\left(\frac{\gamma_{\text{th}}}{\bar{\gamma}}\right)^{\mathcal{N}}, & \text{if} \quad \mathcal{N} = N_S = N_D\frac{\vartheta}{r}. \end{cases} \tag{32}$$

2) *Fixed interference power constraint*: For this scenario, we present the following key result.

*Lemma 6.* The asymptotic outage probability of cognitive sharing with TAS/ARIC of AF multihop relaying network is given by

$$P_{\text{out}}^{\infty}(\gamma_{\text{th}}) \approx \left(\Lambda_1\left(\frac{1}{\mathcal{Q}_P}\right)^{N_S} + \Lambda_2\left(\frac{1}{\mathcal{Q}_I}\right)^{N_S}\right)\gamma_{\text{th}}^{N_S} \tag{33}$$

where $\Lambda_1$ and $\Lambda_2$ are given, respectively, by

$$\Lambda_1 = \sum_{j=0}^{N_S}\binom{N_S}{j}F_{\gamma_g}(\mu)\left[\frac{\bar{\gamma}_1^j}{\Gamma(L_A)}\Gamma\left(L_A+j, \frac{\gamma_{1,T}}{\bar{\gamma}_1}\right) + \frac{\bar{\gamma}_1^j}{\Gamma(L)}\gamma\left(L+j, \frac{\gamma_{1,T}}{\bar{\gamma}_1}\right) + e^{-\gamma_{1,T}/\bar{\gamma}_1}\sum_{h=2}^{N_R}\left(\frac{1}{\bar{\gamma}_1}\right)^{b_5}\frac{\gamma_{1,T}^{b_6}}{(b_6)\Gamma(b_5)}\right] \tag{34}$$

$$\Lambda_2 = \sum_{j=0}^{N_S}\binom{N_S}{j}\left[\frac{\bar{\gamma}_1^j}{\Gamma(L_A)}\Gamma\left(L_A+j, \frac{\gamma_{1,T}}{\bar{\gamma}_1}\right) + \frac{\bar{\gamma}_1^j}{\Gamma(L_T)}\gamma\left(L+j, \frac{\gamma_{1,T}}{\bar{\gamma}_1}\right) + e^{-\gamma_{1,T}/\bar{\gamma}_1}\sum_{h=2}^{N_R}\left(\frac{1}{\bar{\gamma}_1}\right)^{b_5}\frac{\gamma_{1,T}^{b_6}}{(b_6)\Gamma(b_5)}\right]$$

$$\times \Omega_g^{N_S}\frac{L_T}{\Gamma(N)}\sum_{k_3=0}^{L_T-1}\binom{L-1}{k_3}(-1)^{k_3}\Gamma(k_3+1)\sum_{|\mathbf{c}_I|=k_3}\mu_I\frac{\Gamma\left(N_S+\lambda_I+N, \frac{Q_I(k_3+1)}{Q_P\Omega_g}\right)}{(k_3+1)^{(N_S+\lambda_I+N)}}. \tag{35}$$

*Proof:* Follow the same proof adopted in Lemma 2. ∎

For fixed interference power constraint, we obtain the end-to-end asymptotic outage probability of mixed underlay RF/FSO network as follows:

$$P_{\text{out}}^{\infty}(\gamma_{\text{th}}) = \begin{cases} \left(\frac{\left(\frac{1}{\bar{\gamma}}\right)^{N_S}}{1/\Lambda_1} + \frac{\left(\frac{1}{\mathcal{Q}_I}\right)^{N_S}}{1/\Lambda_2}\right)\gamma_{\text{th}}^{N_S}, & \text{if} \quad N_S < N_D\frac{\vartheta}{r} \\ \Pi\left(\frac{\gamma_{\text{th}}}{\bar{\gamma}}\right)^{N_D\frac{\vartheta}{r}}, & \text{if} \quad N_S > N_D\frac{\vartheta}{r} \\ \left(\frac{\Lambda_1+\Pi}{\bar{\gamma}^{\mathcal{N}}} + \frac{\left(\frac{1}{\mathcal{Q}_I}\right)^{\mathcal{N}}}{1/\Lambda_2}\right)\gamma_{\text{th}}^{\mathcal{N}}, & \text{if} \quad \mathcal{N} = N_S = N_D\frac{\vartheta}{r}. \end{cases} \tag{36}$$

## 5. Power Allocation Approach

In this section, a power allocation approach is presented in which two optimization problems are formulated to minimize the asymptotic outage probability of the considered system for DRIC and ARIC models, respectively. For simplicity, without loss of generality, the obtained results for the asymptotic outage probabilities in previous sections are considered as the target functions, and hence, the optimization problem can be formulated as follows

$$\min P_{\text{out}}^{\infty}(\gamma_{\text{th}}), \quad \text{subject to} \quad \begin{cases} P_1 + P_2 = P_T \\ P_1 \leq P_s, \ P_2 \leq P_r \\ \lambda_{k,g}P_1 \leq I_P \end{cases} \tag{37}$$

where $P_T$ is the total allowable power for the dual-hop transmission that must be less than or equal to the sum of the maximum allowable power at each node (i.e., $P_T \leq P_s + P_r$). Based on the discussion

in Section IV, the asymptotic outage probability of the considered model can be re-defined as

$$
P_{\text{out},\mathcal{X}}^{\infty}(\gamma_{\text{th}}) =
\begin{cases}
F_{\gamma_1,\mathcal{X}}^{\infty}(\gamma_{\text{th}}), & \text{if } N_S < N_D \frac{\vartheta}{r} \\
F_{\gamma_1,\mathcal{X}}^{\infty}(\gamma_{\text{th}}) + F_{\gamma_2}^{\infty}(\gamma_{\text{th}}), & \text{if } N_S = N_D \frac{\vartheta}{r} \\
F_{\gamma_2}^{\infty}(\gamma_{\text{th}}), & \text{if } N_S > N_D \frac{\vartheta}{r}
\end{cases}
\tag{38}
$$

where $F_{\gamma_1,\mathcal{X}}^{\infty}(\gamma_{\text{th}})$ and $F_{\gamma_2}^{\infty}(\gamma_{\text{th}})$ denote the asymptotic CDFs of the RF and FSO links, respectively, with $\mathcal{X} \in \{\text{DRIC, ARIC}\}$. It is clear that the maximum asymptotic outage probability case occurs when $\mathcal{N} = N_S = \frac{N_D \vartheta}{r}$. Therefore, we reformulated the target function of the optimization problem such as

$$
\min_{N_S = \frac{N_D \vartheta}{r}} P_{\text{out},\mathcal{X}}^{\infty}(\gamma_{\text{th}}) = \min \left\{ F_{\gamma_1,\mathcal{X}}^{\infty}(\gamma_{\text{th}}) + F_{\gamma_2}^{\infty}(\gamma_{\text{th}}) \right\}
$$

$$
= \min \left\{ \frac{K_1 \gamma_{\text{th}}}{P_1} + \frac{K_2 \gamma_{\text{th}}}{P_2} \right\}.
\tag{39}
$$

It is clear that the function $P_{\text{out},\mathcal{X}}^{\infty}(\gamma_{\text{th}})$ is a convex function as $P_1 \geq 0$ and $P_2 \geq 0$, where $K_1$ and $K_2$ are given, respectively, by

$$
K_1 =
\begin{cases}
\Xi^{\frac{1}{N_S}}, & \text{for DRIC and proportional} \mathcal{Q}_I \\
\Delta_1^{\frac{1}{N_S}}, & \text{for DRIC and fixed} \mathcal{Q}_I \\
\Theta^{\frac{1}{N_S}}, & \text{for ARIC and proportional} \mathcal{Q}_I \\
\Lambda_1^{\frac{1}{N_S}}, & \text{for ARIC and fixed} \mathcal{Q}_I
\end{cases}
\tag{40}
$$

$$
K_2 = \Pi^{\frac{r}{N_D \vartheta}}.
\tag{41}
$$

The constraints can be simplified further by assuming that the maximum allowable power at the SU source (i.e. $P_s$) is higher than $\frac{I_P}{\lambda_g}$, while this assumption can not be valid for the FSO link as the latter's power $P_2$ has to be limited to $P_r$ for eye protection and international regulations. In practice, the laser power $P_r$ is much less than the RF power $P_s$ that cannot be ignored. Then, the problem can be expressed as

$$
\min P_{\text{out}}^{\infty}(\gamma_{\text{th}}), \quad \text{subject to}
\begin{cases}
P_1 + P_2 = P_T \\
P_2 \leq P_r \\
\lambda_g P_1 \leq I_P.
\end{cases}
\tag{42}
$$

Using Lagrangian multiplier method, we obtain the Lagrangian function:

$$
\mathcal{J}(P_1, P_2, \nu, \epsilon_1, \epsilon_2) = \frac{K_1 \gamma_{\text{th}}}{P_1} + \frac{K_2 \gamma_{\text{th}}}{P_2} + \nu(P_1 + P_2 - P_T)
$$

$$
+ \epsilon_1 (\lambda_g P_1 - I_P) + \epsilon_2 (P_2 - P_r)
\tag{43}
$$

where $\nu$, $\epsilon_1$, and $\epsilon_2$ are Lagrangian multipliers. According to the Karush-Kuhn-Tucker (KKT) conditions, we obtain the following:

$$
\frac{\partial \mathcal{J}(P_1, P_2, \nu, \epsilon_1, \epsilon_2)}{\partial P_1} = 0
\tag{44a}
$$

$$
\frac{\partial \mathcal{J}(P_1, P_2, \nu, \epsilon_1, \epsilon_2)}{\partial P_2} = 0
\tag{44b}
$$

$$
\nu(P_1 + P_2 - P_T) = 0
\tag{44c}
$$

$$
\epsilon_1 (\lambda_g P_1 - I_P) = 0
\tag{44d}
$$

$$
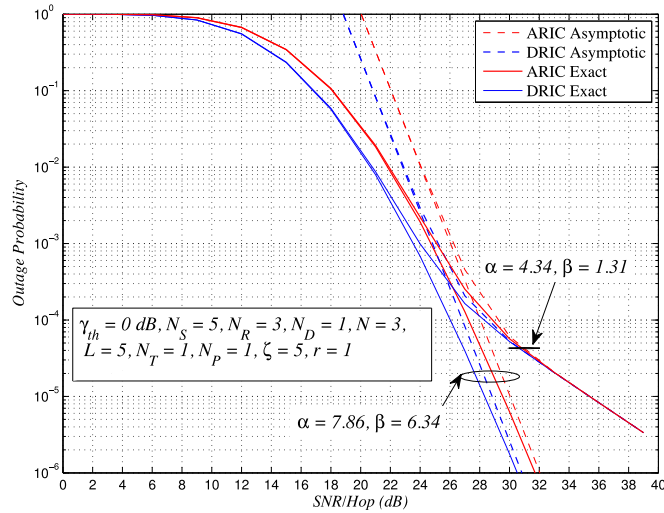\epsilon_2 (P_2 - P_r) = 0.
\tag{44e}
$$

Fig. 2. Outage probability for DRIC and ARIC schemes versus SNR for different atmospheric turbulence conditions.

Then, through the simultaneous solution of the equations we obtain the optimal power allocation $P_1^*$ that is given by

$$
P_1^* = \begin{cases}
\frac{I_P}{\lambda_g}, & \text{if} \quad P_T \geq \frac{I_P}{\lambda_g} + P_r \\
\frac{I_P}{\lambda_g}, & \text{if} \quad \mathcal{L}_1 < P_T < \frac{I_P}{\lambda_g} + P_r, \text{ and } \mathcal{L}_1 = \min\left(\mathcal{L}_1, \mathcal{L}_2\right) \\
P_T - P_r, & \text{if} \quad \mathcal{L}_2 < P_T < \frac{I_P}{\lambda_g} + P_r, \text{ and } \mathcal{L}_2 = \min\left(\mathcal{L}_1, \mathcal{L}_2\right) \\
\frac{\sqrt{\frac{K_1}{K_2}} P_T}{1 + \sqrt{\frac{K_1}{K_2}}}, & \text{if} \quad 0 < P_T < \min(\mathcal{L}_1, \mathcal{L}_2)
\end{cases}
\tag{45}
$$

where $P_2^*$ is obtained by using $P_2^* = P_T - P_1^*$, $\mathcal{L}_1 = (1 + \sqrt{\frac{K_2}{K_1}})\frac{I_P}{\lambda_g}$, and $\mathcal{L}_2 = (1 + \sqrt{\frac{K_1}{K_2}})P_r$. It can be noticed that the optimal power allocation has different solutions according to different $P_T$ values.

## 6. Numerical Results and Simulations

In this section, some numerical results are presented with Monte Carlo simulations to validate the derived expressions. The numerical results investigate the impact of some key parameters such as the number of SUs, the number of antennas, and the atmospheric turbulence conditions on the system outage performance for ICs schemes. Moreover, the effect of the proposed power allocation approach on the system performance is discussed for both DRIC and ARIC schemes.

In Fig. 2, the impact of the atmospheric turbulence conditions on the system outage probability for both DRIC and ARIC schemes is investigated. The results study two cases that are the strong turbulence case (i.e., $\alpha = 4.34$ and $\beta = 1.31$) and the weak turbulence case (i.e., $\alpha = 7.86$ and $\beta = 6.34$). In low to medium SNR values, it can be noticed that the system outage performance for both DRIC and ARIC is not affected by the atmospheric turbulence conditions and each scheme has an identical performance in both cases. However, at high SNR values, both schemes are affected by the strong turbulence conditions that results in degrading their outage performance compared to the weak turbulence case. Moreover, it is clear that the performance of DRIC scheme outperforms the ARIC scheme. However, at high SNR values in the case of strong turbulence conditions, both schemes provide the same outage performance as the FSO link in this case dominates the system performance that kills any advantage for the DRIC scheme over the ARIC scheme.
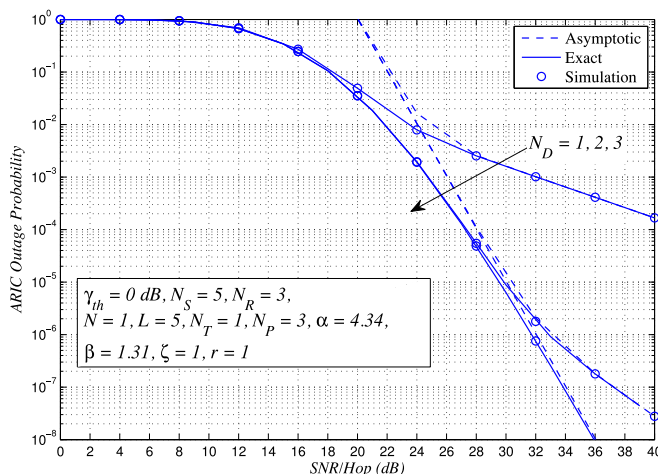
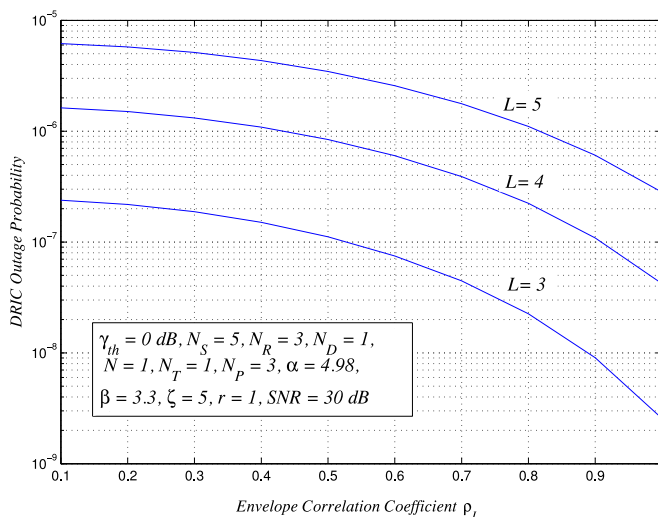Fig. 3. Outage probability of ARIC scheme versus SNR for different number of destinations $N_D$.



Fig. 4. Outage probability of DRIC scheme versus envelop correlation coefficient $\rho_I$ for different number of PU sources $L$.

In Fig. 3, the ARIC outage performance is investigated for different number of SU destinations at strong turbulence conditions. The results show that increasing the number of SU destination improves the system outage probability and enhances the diversity order of the considered system. It can be noticed that at low to medium SNR values, increasing $N_D$ does not enhance the system outage performance as the system performance in this region is dominated by the RF links that are independent of $N_D$. However, at the high SNR values, increasing $N_D$ enhances the system outage probability as the system in this region is dominated by the FSO links that depend on $N_D$. Moreover, the figure shows that the derived exact and asymptotic expressions match the Monte Carlo simulations results that validate the analysis.

In Fig. 4, the effect of the envelop correlation coefficient $\rho_I$ on the outage performance of the considered system with DRIC scheme is investigated. The results show that an increase in $\rho_I$ enhances the system outage performance as the dominant interferer is more correlated with other interferer's that enhances the interference cancellation operation. Moreover, it can be noticed that increasing the number of PU sources $L$ degrades the system outage performance by increasing the number of interferer's at the relay antennas.
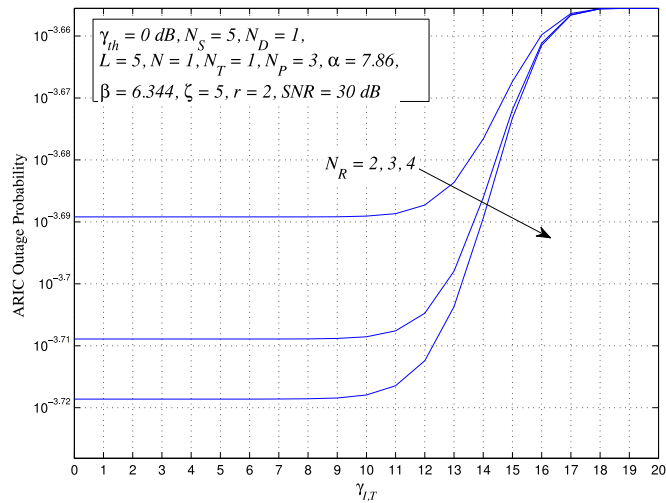
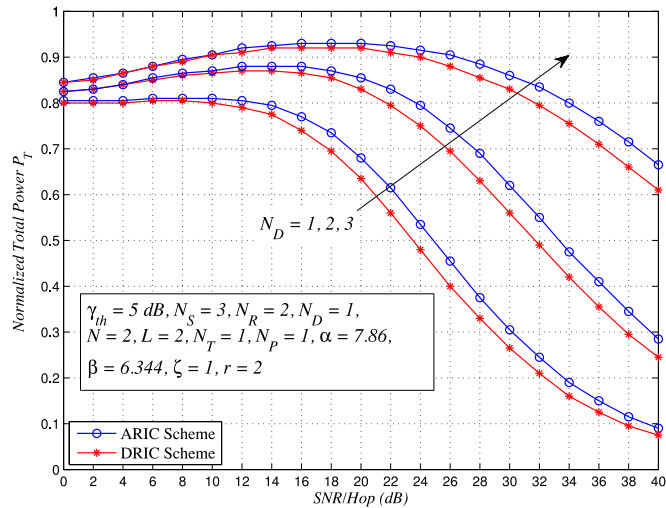Fig. 5. Outage probability of ARIC scheme versus $\gamma_{I,T}$ for different number of SU relay antennas $N_R$.



Fig. 6. Optimal RF power versus SNR for different number of SU destinations $N_D$.

For ARIC scheme, the impact of $\gamma_{I,T}$ on the outage performance of the considered system is analyzed in Fig. 5. The result show that increasing $\gamma_{I,T}$ degrades the system outage performance, as expected. Moreover, the results demonstrate that increasing the number of relay antennas $N_R$ enhances the system performance and increases its diversity.

Fig. 6 depicts the optimal power allocation solutions of the proposed power allocation approach for both DRIC and ARIC schemes. It is clear that for each SNR value the optimal RF power for the DRIC scheme is always less than that of the ARIC scheme since the performance of the DRIC scheme is always better than the ARIC scheme as shown previously. Moreover, at high SNR values, the results show that the optimal RF power decreases as most of the total power is used to enhance the RF link that suffers from strong turbulence conditions. However, we can notice that increasing the number of SU destinations $N_D$ enhances the FSO link performance, resulting in reducing the need of optical power and pumps more power on the RF link to minimize the total outage probability.

In Fig. 7, the impact of the misalignment between the optical transmitter and receiver $\xi$ on the optimal solution of the power allocation approach is studied. The results show that increasing $\xi$, which reflects a good alignment between the two optical nodes, enhances the FSO link performance
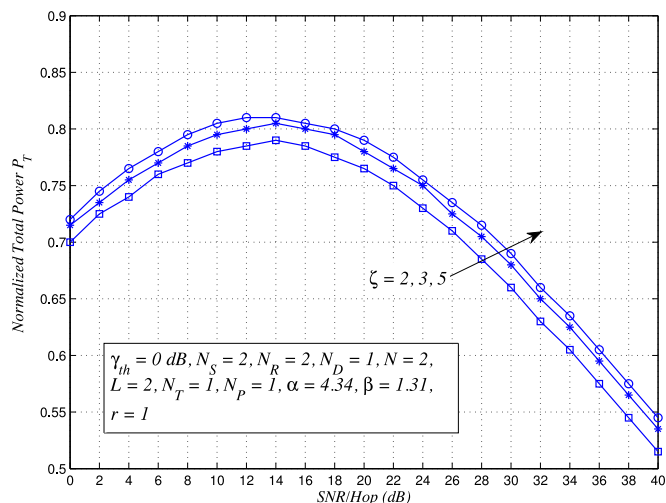
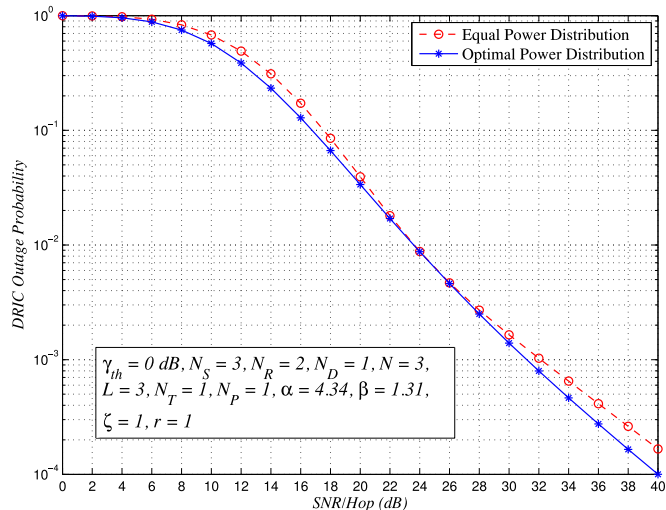Fig. 7. Optimal RF power versus SNR for different values of $\xi$.



Fig. 8. Outage probability of DRIC scheme versus SNR for both equal power and optimal power distribution models.

and reduces the need of optical power. As a result, increasing $\xi$ increases the optimal RF power allocated for the RF link to minimize the system outage probability.

The impact of the equal power distribution and the optimal power distribution model on the outage performance of the considered system with DRIC scheme is investigated in Fig. 8. The results show that the performance of the proposed power allocation approach outperforms that of the equal power distribution model. The results emphasize the importance of the proposed power allocation approach that can be utilized to wisely distribute the total power budget between the RF and FSO links to ensure minimum outage probability.

## 7. Conclusion

This paper has developed new analytical models that can be used to investigate the outage performance of a mixed relaying communication with an underlay cognitive RF MIMO and a multi-destination FSO and employing different receive IC at the relaying node. The adopted system and

channel models have been incorporated into extensive analytical developments that have led to closed-form expressions for the system outage performance. These results can be used to investigate the effects of cognitive radio power and interference limitations, the receive IC scheme at the relay node, the number of multiuser RF sources, the number of FSO destinations, and the effects of pointing errors and detection technique on the FSO link on the achieved system outage performance. In addition, simple expressions for the end-to-end outage probability in the high SNR regime have been derived, which have been used to clarify the system diversity and coding gains for various scenarios of the system and channel parameters. Our results reveal that under weak atmospheric turbulence conditions, the system performance is dominated by RF channel, and hence a maximum diversity gain is achieved when the peak interference power constraint $\mathcal{Q}_I$ is proportional to the maximum transmit power $\mathcal{Q}_P$. On the other hand, under severe atmospheric turbulence conditions, the system performance is dominated by the FSO channel, hence the diversity gain is a result of the minimum value of the turbulence fading and pointing error parameters.

# Appendix

## 7.1 Proof of Lemma 1

In the following, we derive the CDF of $\gamma_{1,\text{DRIC}}$ of (3) as follows:

$$F_{\gamma_{1,\text{DRIC}}}(\gamma_{\text{th}}) = \Pr\left( \min\left( \frac{\mathcal{Q}_I}{\lambda_g}, \mathcal{Q}_P \right) \frac{\lambda_h}{\gamma_{1,\text{tot}} + 1} \leq \gamma_{\text{th}} \right). \tag{46}$$

To proceed with the analysis, we need to average over the distributions of $\gamma_{1,\text{tot}}$, $\lambda_g$ as

$$F_{\gamma_{1,\text{DRIC}}}(\gamma_{\text{th}}) = \underbrace{\Pr\left\{ \frac{\mathcal{Q}_P \lambda_h}{\gamma_{1,\text{tot}} + 1} \leq \gamma_{\text{th}}, \mathcal{Q}_P \leq \frac{\mathcal{Q}_I}{\lambda_g} \right\}}_{\mathcal{I}_1}$$
$$+ \underbrace{\Pr\left\{ \frac{\mathcal{Q}_I \lambda_h}{\lambda_g (\gamma_{1,\text{tot}} + 1)} \leq \gamma_{\text{th}}, \frac{\mathcal{Q}_I}{\lambda_g} \leq \mathcal{Q}_P \right\}}_{\mathcal{I}_2}. \tag{47}$$

The first summand can be evaluated as

$$\mathcal{I}_1 = F_{\lambda_g}\left( \frac{\mathcal{Q}_I}{\mathcal{Q}_P} \right) \int_0^\infty F_{\lambda_h}\left( \frac{\gamma_{\text{th}}(z + 1)}{\mathcal{Q}_P} \right) f_{\gamma_{1,\text{tot}}}(z) dz. \tag{48}$$

With the appropriate substitutions of the distributions of $\lambda_g$ and $\gamma_{1,\text{tot}}$ into (48), and with the help of [29, 3.351.3], the term $\mathcal{I}_1$ can be evaluated in closed-form expression. For $\mathcal{I}_2$, we have

$$\mathcal{I}_2 = \int_0^\infty \left( \int_{\frac{\mathcal{Q}_I}{\mathcal{Q}_P}}^\infty F_{\lambda_h}\left( \frac{\gamma_{\text{th}} y (z + 1)}{\mathcal{Q}_I} \right) f_{\lambda_{l,g}}(y) dy \right) f_{\gamma_{1,\text{tot}}} dz. \tag{49}$$

Starting with the inner integral, by performing appropriate substitution of $\lambda_h$ into (49) and averaging over the distribution of $\lambda_g$, the integral can be evaluated in closed-form with the help of [29, 3.351.3]. Then the outer integral can be solved by averaging over the distribution $\gamma_{k,l,\text{tot}}$. Next, with a careful mathematical manipulation and applying [29, 3.471.7], the final solution of $l_2$ is obtained.

## 7.2 Proof of Lemma 2

For ARIC scenario, we follow the same steps as developed in *Lemma* 1 to derive $\gamma_{1,\text{DRIC}}$ for the DRIC scenario. Therefore, we need to evaluate $\gamma_{2,\text{ARIC}}$ by re-expressing $\mathcal{I}_1$ and $\mathcal{I}_2$ in (48) and (49), respectively, for ARIC scheme. The only difference from *Lemma* 1 is to average over the distribution of ARIC as expressed in (11) instead of the distribution of DRIC as in (9). Therefore, the integral

term $\mathcal{I}_1$ can be expressed as

$$\mathcal{I}_1 = F_{\lambda_g}\left(\frac{\mathcal{Q}_I}{\mathcal{Q}_P}\right)\int_{\gamma_{,T}}^{\infty} F_{\lambda_h}\left(\frac{\gamma_{\text{th}}(z+1)}{\mathcal{Q}_P}\right)f_{\gamma_{I,\text{tot}}}^{z>\gamma_{,T}}(z)dz$$

$$+\int_0^{\gamma_{,T}} F_{\lambda_{k,h}}\left(\frac{\gamma_{\text{th}}(z+1)}{\mathcal{Q}_P}\right)f_{\gamma_{I,\text{tot}}}^{z\le\gamma_{,T}}(z)dz \tag{50}$$

where $f_{\gamma_{I,\text{tot}}}^{z>\gamma_{,T}}(z)$ and $f_{\gamma_{I,\text{tot}}}^{z\le\gamma_{,T}}(z)$ are given, respectively, by

$$f_{\gamma_{I,\text{tot}}}^{z>\gamma_{,T}}(z) = \frac{1}{\Gamma(L_A)}\left(\frac{1}{\overline{\gamma}_I}\right)^{L_A} z^{L_A-1}e^{-z/\overline{\gamma}_I} \tag{51}$$

and

$$f_{\gamma_{I,\text{tot}}}^{z\le\gamma_{,T}}(z) = \frac{1}{\Gamma(L)}\left(\frac{1}{\overline{\gamma}_I}\right)^{L} z^{L-1}e^{-z/\overline{\gamma}_I}$$

$$+ e^{-\gamma_{,T}/\overline{\gamma}_I}\sum_{h=2}^{L_R}\frac{\left(\frac{1}{\overline{\gamma}_I}\right)^{\iota}}{\Gamma(\iota)}z^{\iota-1}. \tag{52}$$

On appropriately substituting the distributions of $\lambda_g$ and $\gamma_{I,\text{tot}}$ into (48) and utilizing [29, 3.381.1] and [29, 3.381.2], the first and second integrals are evaluated in closed-from expressions, respectively. After evaluating $\mathcal{I}_1$, we turn our attention to $\mathcal{I}_2$, and we have

$$\mathcal{I}_2 = \int_0^{\infty}\left(\int_{\frac{\mathcal{Q}_I}{\mathcal{Q}_P}}^{\infty} F_{\lambda_h}\left(\frac{\gamma_{\text{th}}y(z+1)}{\mathcal{Q}_I}\right)f_{\lambda_{I,g}}(y)dy\right)f_{\gamma_{I,\text{tot}}}(z)dz. \tag{53}$$

Starting with the inner integral, by performing appropriate substitution of $\lambda_h$ into (53) and averaging it over the distribution of $\lambda_g$, the inner integral i.e., $\mathcal{I}_3$ integral is evaluated in closed-form with the help of [29, 3.351.3] as

$$\mathcal{I}_3 = \frac{L}{\Gamma(N)\Omega_{k,g}}\sum_{k_1=0}^{N_S}\binom{N_S}{k_1}(-1)^{k_1}\sum_{k_3=0}^{L-1}\binom{L-1}{k_3}\frac{\Gamma(k_3+1)}{(-1)^{-k_3}}$$

$$\times\sum_{|\mathbf{c_I}|=k_3}\mu_I\left(\frac{1}{\Omega_g}\right)^{\lambda_I+N-1}\exp\left(-\frac{Q_I}{Q_P}\phi\right)\sum_{k=0}^{\mu_2-1}\frac{\Gamma(\mu_2)}{\Gamma(k+1)}$$

$$\times\left(\frac{Q_I}{Q_P}\right)^k\left(\frac{1}{\phi}\right)^{\mu_2-k}\frac{\exp\left(-\frac{Q_I k_1\theta}{Q_P}z\right)}{\left(1+\frac{k_1\theta}{\phi}z\right)^{(\mu_2-k)}}. \tag{54}$$

Then, the outer integral can be solved by averaging over the distribution $\gamma_{k,I,\text{tot}}$ as

$$\mathcal{I}_2 = \frac{L}{\Gamma(N)\Omega_g}\sum_{k_1=0}^{N_S}\binom{N_S}{k_1}(-1)^{k_1}\sum_{k_3=0}^{L-1}\binom{L-1}{k_3}\frac{\Gamma(k_3+1)}{(-1)^{-k_3}}$$

$$\times\sum_{|\mathbf{c_I}|=k_3}\mu_I\left(\frac{1}{\Omega_{k,g}}\right)^{\lambda_I+N-1}\exp\left(-\frac{Q_I}{Q_P}\phi\right)\sum_{k=0}^{\mu_2-1}\frac{\Gamma(\mu_2)}{\Gamma(k+1)}$$

$$\times \left(\frac{Q_I}{Q_P}\right)^k \left(\frac{1}{\phi}\right)^{\mu_2-k} \left( \int_0^{\gamma_{I,T}} \frac{\exp\left(-\frac{Q_I k_1 \theta}{Q_P} z\right)}{\left(1+\frac{k_1 \theta}{\phi} z\right)^{(\mu_2-k)}} f_{\gamma_{k,I,\text{tot}}}^{z \leq \gamma_{I,T}}(z) dz \right.$$

$$\left. + \int_{\gamma_{I,T}}^{\infty} \frac{\exp\left(-\frac{Q_I k_1 \theta}{Q_P} z\right)}{\left(1+\frac{k_1 \theta}{\phi} z\right)^{(\mu_2-k)}} f_{\gamma_{I,\text{tot}}}^{z \leq \gamma_{I,T}}(z) \right). \tag{55}$$

To evaluate the above integrals, we perform change of variable $u = (1 + \frac{k_1 \theta}{\phi} z)$ and on applying [29, 3.471.7], the final solution of $\mathcal{I}_2$ is obtained. To this end, after evaluating $\mathcal{I}_1$ and $\mathcal{I}_2$, the desired results for *Lemma* 2 are obtained.

## References

[1] L. C. Andrews, R. L. Phillips, and C. Y. Hopen, "Laser beam scintillation with applications," Bellingham, WA, USA: SPIE, 2001.

[2] H. Samimi, "Optical communication using subcarrier intensity modulation through generalized turbulence channels," *IEEE/OSA J. Opt. Commun. Netw.*, vol. 4, no. 5, pp. 378–381, May 2012.

[3] D. Kedar and S. Arnon, "Urban optical wireless communication networks: The main challenges and possible solutions," *IEEE Commun. Mag.*, vol. 42, no. 5, pp. S2–S7, May 2004.

[4] I. S. Ansari, F. Yilmaz, and M.-S. Alouini, "Performance analysis of free-space optical links over Málaga ($\mathcal{M}$) turbulence channels with pointing errors," *IEEE Trans. Wireless Commun.*, vol. 15, no. 1, pp. 91–102, Jan. 2016.

[5] I. F. Akyildiz, W.-Y. Lee, M. C. Vuran, and S. Mohanty, "Next generation dynamic spectrum access cognitive radio wireless networks: A survey," *Comput. Netw.*, vol. 50, no. 13, pp. 2127–2159, Sep. 2006.

[6] Q. Zhao and B. M. Sadler, "A survey of dynamic spectrum access," *IEEE Signal Process. Mag.*, vol. 24, no. 3, pp. 79–89, May 2007.

[7] A. Ghasemi and E. S. Sousa, "Fundamental limits of spectrum-sharing in fading environments," *IEEE Trans. Wireless Commun.*, vol. 9, no. 2, pp. 649–658, Feb. 2007.

[8] J. Lee, H. Wang, J. G. Andrews, and D. Hong, "Outage probability of cognitive relay networks with interference constraints," *IEEE Trans. Wireless Commun.*, vol. 10, no. 2, pp. 390–395, Feb. 2011.

[9] C. Zhong, T. Ratnarajah, and K.-K. Wong, "Outage analysis of decode-and-forward cognitive dual-hop systems with the interference constraint in Nakagami-$m$ fading channels," *IEEE Trans. Veh. Technol.*, vol. 60, no. 6, pp. 2875–2879, Jul. 2011.

[10] W. Xu, J. Zhang, P. Zhang, and C. Tellambura, "Outage probability of decode-and-forward cognitive relay in presence of primary user's interference," *IEEE Commun. Lett.*, vol. 16, no. 8, pp. 1252–1255, Aug. 2012.

[11] T. Q. Duong, D. B. da Costa, T. A. Tsiftsis, C. Zhong, and A. Nallanathan, "Outage and diversity of cognitive relaying systems under spectrum sharing environments in Nakagami-$m$ fading," *IEEE Commun. Lett.*, vol. 16, no. 12, pp. 2075–2078, Dec. 2012.

[12] F. S. Al-Qahtani, Yu. Huangm, M. Di Renzo, S. Ikki, and H. Alnuweiri, "Space shift keying (SSK-) MIMO of spectrum sharing network over Rayleigh fading channels," *IEEE Commun. Lett.*, vol. 16, no. 9, pp. 1503–1506, Jul. 2014.

[13] I. S. Ansari, M. M. Abdallah, M.-S. Alouini, and K. A. Qaraqe, "Outage performance analysis of underlay cognitive RF and FSO wireless channels," *in Proc. 3rd Int. Workshop Opt. Wireless Commun.*, Funchal, Madeira Islands, Portugal, Sep. 2014, pp. 6–10.

[14] I. S. Ansari, M. M. Abdallah, M.-S. Alouini, and K. A. Qaraqe, "A performance study of two hop transmission in mixed underlay RF and FSO fading channels," *in Proc. IEEE Wireless Commun. Netw. Conf.*, Istanbul, Turkey, Apr. 2014, pp. 388–393.

[15] M. O. Hasna, M.-S. Alouini, A. Bastami, and E. S Ebbini, "Performance analysis of cellular mobile radio systems with successive co-channel interference cancellation," *IEEE Trans. Wireless Commun.*, vol. 2, no. 1, pp. 29–49, Jan. 2003.

[16] R. M. Radaydeh and M.-S. Alouini, "Adaptive co-channel interference cancelation for power-limited applications," *in Proc. IEEE Int. Symp. Personal, Indoor Mobile Radio Commun.*, Istanbul, Turkey, Sep. 2010, pp. 521–526.

[17] R. M. Radaydeh and M.-S. Alouini, "Performance analysis of power-efficient adaptive interference cancelation in fading channels," *in Proc. IEEE Global Telecomm. Conf.*, 2010, pp. 1–5.

[18] S. S. Ikki and S. Aissa, "Multihop wireless relaying systems in the presence of co-channel interference: Performance analysis and design optimization," *IEEE Trans. Veh. Technol.*, vol. 61, no. 2, pp. 566–573, Feb. 2012.

[19] B. Allen and M. Ghavami, *Adaptive Array Systems: Fundamentals and Applications*. New York, NY, USA: Wiley, 2005.

[20] J. A. Ritcey and M. Azizoglu, "Performance analysis of generalized selection combining with switching constraints," *IEEE Commun. Lett.*, vol. 4, pp. 152–154, May 2000.

[21] J. N. Laneman, D. N. C. Tse, and G. W. Wornell, "Cooperative diversity in wireless networks: Efficient protocols and outage behavior," *IEEE Trans. Inf. Theory*, vol. 50, no. 12, pp. 3062–3080, Dec. 2004.

[22] E. Bayaki, R. Schober, and R. K. Mallik, "Performance analysis of MIMO free-space optical systems in Gamma-Gamma fading," *IEEE Trans. Commun.*, vol. 57, no. 11, pp. 3415–3424, Nov. 2009.

[23] K. P. Peppas, "A simple, accurate approximation to the sum of Gamma-Gamma variates and applications in MIMO free-space optical systems," *IEEE Photon. Technol. Lett.*, vol. 23, no. 13, pp. 839–841, Jul. 2011.

[24] L. Yang, M. O. Hasna, and X. Gao, "Performance of mixed RF/FSO with variable gain over generalized atmospheric turbulence channels," *IEEE J. Select. Areas Commun.*, vol. 33, no. 9, pp. 1913–1924, Sep. 2015.

[25] A. Farid and S. Hranilovic, "Outage capacity optimization for free-space optical links with pointing errors," *IEEE/OSA J. Lightw. Technol.*, vol. 25, no. 7, pp. 1702–1710, Jul. 2007.

[26] M. I. Petkovic, A. M. Cvetkovic, G. T. Djordjevic, and G. K. Karagiannidis, "Partial relay selection with outdated channel state estimation in mixed RF/FSO systems," *IEEE/OSA J. Lightw. Technol.*, vol. 33, no. 13, pp. 2860–2867, Mar. 2015.

[27] R. M. Radaydeh and M.-S. Alouini, "On the performance of arbitrary transmit selection for threshold-based receive MRC with and without co-channel Interference," *IEEE Trans. Commun.*, vol. 59, no. 11, pp. 3177–3191, Nov. 2011.

[28] S. Choi and Y.-C. Ko, "Performance of selection MIMO systems with generalized selection criterion over Nakagami-m fading channels," *IEICE Trans. Commun.*, vol. E89-B, pp. 3467–3470, Dec. 2006

[29] I. S. Gradshteyn and I. M. Ryzhik, *Table of Integrals, Series and Products*. 6th ed. San Diego, CA, USA: Academic, 2000.